Viscoelasticity of Single Wall Carbon Nanotube Suspensions

L. A. Hough,[1] M. F. Islam,[1] P. A. Janmey,[2] and A. G. Yodh[1]

[1]*Department of Physics and Astronomy, University of Pennsylvania, Philadelphia, Pennsylvania 19104-6396, USA*
[2]*Institute of Medicine and Engineering, University of Pennsylvania, Philadelphia, Pennsylvania 19104-6383, USA*

(Received 23 May 2004; published 13 October 2004)

We investigate the viscoelastic properties of an associating rigid rod network: aqueous suspensions of surfactant stabilized single wall carbon nanotubes (SWNTs). The SWNT suspensions exhibit a rigidity percolation transition with an onset of solidlike elasticity at a volume fraction of 0.0026; the percolation exponent is 2.3 ± 0.1. At large strain, the solidlike samples show volume fraction dependent yielding. We develop a simple model to understand these rheological responses and show that the shear dependent stresses can be scaled onto a single master curve to obtain an internanotube interaction energy per bond $\approx 40k_BT$. Our experimental observations suggest SWNTs in suspension form interconnected networks with bonds that freely rotate and resist stretching. Suspension elasticity originates from bonds between SWNTs rather than from the stiffness or stretching of individual SWNTs.

DOI: 10.1103/PhysRevLett.93.168102 PACS numbers: 83.80.Hj, 82.70.–y, 87.15.La

The mechanical properties of associating semiflexible polymer and rod networks play a critical role in a variety of materials' contexts ranging from cross-linked actin gels [1] to stress-bearing colloidal suspensions [2,3] and polymeric composites [4–6]. Generally, the rheology of these networks depends on many factors, including the bonds between rods, rod concentration, and rod flexibility. The relationship, however, between the microscopic structure and the macroscopic elasticity of *associating* networks of stiff rods remains essentially unexplored.

In this Letter, we investigate the viscoelasticity of an associating rigid rod network: aqueous suspensions of surfactant stabilized single wall carbon nanotubes (SWNTs). SWNTs have lengths ranging from 100 nm to a few microns, diameters of $\sim$1 nm, and a persistence length $l_p \sim 22\ \mu$m [7]. The attraction between bare SWNTs due to van der Waals interaction is very strong, $\sim 40k_BT$/nm [9]. By coating SWNTs with sodium dodecyl benzene sulfonate (NaDDBS) [10], we have been able to create stable SWNT suspensions that form networks at large concentrations, presumably because the nanotubes form physical bonds with each other along contacting nanotube segments. The resultant suspensions provide a fascinating model system, wherein intertube bonding contributes substantially to the network elasticity. This system contrasts well with cross-linked actin networks, wherein the elasticity originates from the bending or stretching of individual filaments [1]. Our measurements are also of potential importance for nanotube materials processing. SWNTs in isolation possess remarkable mechanical, electrical, and thermal properties [8,11,12], and, as a result, networks of nanotubes have been used as a basis for electrically conductive and mechanically tough composites [4,5]. The experiments herein provide a new rheological understanding about solutions of SWNTs, which may improve our ability to control the processing precursors of these novel composites.

We find that SWNT suspensions form elastic solids above a characteristic volume fraction, and we interpret this transition as rigidity percolation. The percolation exponent is obtained from the dependence of network elasticity on rod volume fraction, and comparison with bond percolation simulations [13] suggests the bonds between SWNTs freely rotate but resist stretching. All of the solidlike suspensions exhibit volume fraction dependent yielding at high strain, presumably due to breaking of bonds and network reorganization. We introduce a simple microscopic model that scales out the volume fraction dependencies of the stress-strain curves, thus collapsing all data onto a single master curve. The scaling behavior reveals the dominant contribution to the elasticity of the networks is from the bonds between the SWNTs. The master curve also allows us to estimate the bond energy between SWNTs as $\approx 40k_BT$, in good agreement with prediction [9].

SWNTs are obtained in raw form from Carbon Nanotechnologies Inc. (HiPCO). After purification [14], the material contains >90% SWNTs. The nanotubes have an average diameter $D = 1.1 \pm 0.2$ nm and an average length $L = 165 \pm 80$ nm [10]. To prepare SWNT suspensions of volume fraction $\phi \leq 0.001$, we disperse purified SWNTs in water with NaDDBS surfactant ($C_{12}H_{25}C_6H_4SO_3Na$) and bath sonicate the suspensions for 16–24 h. We obtain SWNT suspensions of $\phi > 0.001$ by ultracentrifuging a suspension of $\phi = 0.001$ at 340 000 g to sediment the surfactant stabilized SWNTs. We then high-shear mix sedimented SWNTs with NaDDBS solutions to prepare suspensions of various concentrations. The concentration ratio of SWNTs to NaDDBS is 1:5 by weight for all SWNT suspensions [10]. Bundling of SWNTs was quantified by diluting concentrated sample with water and performing atomic force microscopy measurements [10]. All SWNT suspensions were composed of 55% to 75% single tubes; the remainder contained small bundles with diameters less

than 5 nm [10]. Neutron scattering studies also showed SWNTs behave like rigid rods in suspension [15]. Even though the SWNTs are coated with surfactant, the suspensions form elastic solids at concentrations above the SWNT overlap concentration [16] within 24 h after preparation.

We measured the viscoelastic properties of SWNT suspensions using a Bohlin Gemini stress controlled rheometer, Fig. 1 (inset). The samples were loaded between 40 mm diameter parallel plates with a 250 μm gap and were allowed to equilibrate for 1 h. We did not prestress the SWNT suspensions because prestressing can align the SWNTs along the shear-flow direction. In addition, prestressing the samples would have required leaving the samples undisturbed between the parallel plates for $\sim$24 h to equilibrate; this delay always induced drying of the samples. During the measurements, we used a solvent trap and a sample cover to avoid excessive drying.

To elucidate relaxation dynamics, we measure the volume fraction ϕ dependent viscoelastic storage G' and loss G'' moduli as a function of oscillation frequency ω at a strain amplitude ϵ of 0.01 (see Fig. 1). At $\phi = 0.0025$, G' and G'' drop below the machine sensitivity of 1 m Pa, and for $\phi \geq 0.003$, G' and G'' are nearly independent of ω. The dominance of G' over G'' across the accessible frequency range indicates the network relaxation time is longer than experimentally accessible. A long relaxation time implies the bonds between the nanotubes prevent thermally induced structural relaxation of the material.

The elastic shear modulus at small frequencies is defined as the plateau modulus G'_0 and is plotted as a function of ϕ in Fig. 2. We interpret the greater than 2 orders of magnitude jump in G'_0 for ϕ between 0.0025 and 0.003 as rigidity percolation. Near the percolation threshold, $G'_0 \propto (\phi - \phi^*)^\nu$, where ϕ^* is the percolation volume fraction, and ν is the percolation exponent. By varying ϕ^* to minimize the error in the slope of a double log plot of G'_0 versus $(\phi - \phi^*)$ (see Fig. 2, inset), we obtain $\phi^* = 0.0026$, approximately twice the estimated overlap volume fraction $\bar{\phi} = 0.0014$ [16]. This higher concentration is sensible since two rods are the minimum number needed to form a connected element (corresponding to $\bar{\phi}$), but at least three rods are needed to form a stress-bearing structure [18].

We determine a percolation exponent $\nu = 2.3 \pm 0.1$ from the slope of the double log plot of G'_0 versus $(\phi - \phi^*)$ [19]. A percolation exponent of 2.1 ± 0.2 has been reported for simulations of percolating bonds that resist stretching but are free to rotate [13]. In contrast, an exponent of 3.75 ± 0.11 is predicted for bonds that resist stretching and rotating [13]. Recent simulations have suggested that rigidity percolation of semiflexible rods can be explained in terms of the bending of the filaments (nonaffine deformation) [20–22]. Although we do not entirely rule out the possibility that SWNT suspensions belong to this new class, the absence of a three-dimensional theory and the SWNT stiffness [7] motivate us to interpret the results as central force bond percolation [13]. Thus our measurements of linear elasticity suggest SWNT networks are composed of freely jointed, associating rods.

The microscopic structure of the SWNT network is revealed through measurements of nonlinear rheological responses. To this end, G' and G'' at 1 Hz are shown in Fig. 3(a) as a function of strain amplitude ϵ and volume fraction ϕ. The SWNT suspensions do not show strain hardening, analogous to cross-linked actin solutions [1]; rather they exhibit strain weakening and a characteristic ϕ dependent yield strain [23]. The loss modulus also shows a slight upturn before fluidization. Many soft materials exhibit similar nonlinear viscoelastic responses [24]. However, unlike SWNT suspensions, the yield strain for such materials is typically *independent* of ϕ. We find empirically it is possible to eliminate the ϕ dependence of the strain by multiplying ϵ by a scale factor proportional to $(\phi - \phi^*)^{1/2}$ [see Fig. 3(b)]. This shifts the

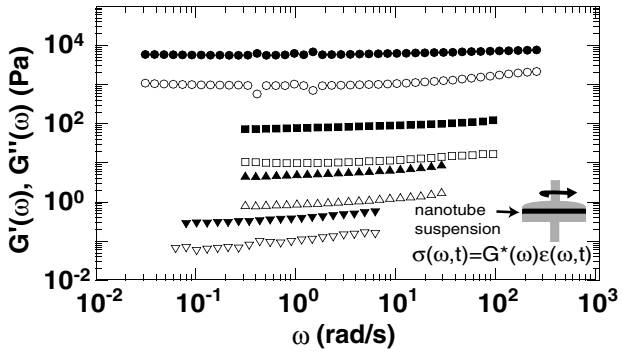

FIG. 1. The volume fraction ϕ dependent viscoelastic storage G' (solid symbols) and loss G'' (open symbols) moduli versus oscillation frequency ω for SWNT suspensions (circles, $\phi = 0.03$; squares, $\phi = 0.0075$; up triangles, $\phi = 0.004$; down triangles, $\phi = 0.003$). Inset: A schematic of the rheometer. The components of the complex shear modulus $G^*(\omega) = G'(\omega) + iG''(\omega)$ are obtained from measurements of the in-phase and the out-of-phase components of the shear stress σ with respect to an oscillatory strain ϵ.

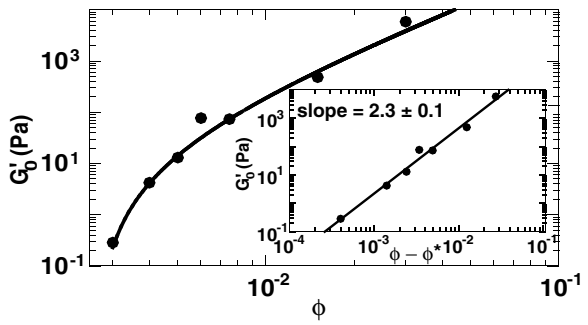

FIG. 2. The storage plateau modulus G'_0, obtained at 1 Hz, versus volume fraction ϕ of SWNT suspensions. Inset: G'_0 versus the reduced volume fraction $(\phi - \phi^*)$.

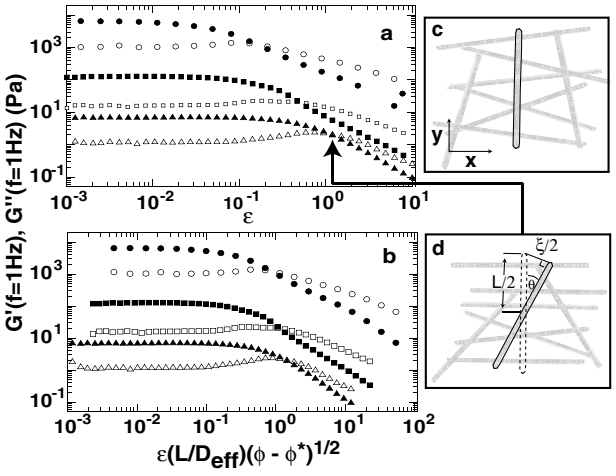

FIG. 3. (a) The volume fraction ϕ dependent storage G' (solid symbols) and loss G'' (open symbols) moduli versus strain amplitude ϵ at 1 Hz for SWNT suspensions (circles, $\phi = 0.03$; squares, $\phi = 0.0075$; up triangles, $\phi = 0.004$). (b) G' and G'' as a function of scaled ϵ, for various ϕ. (c) A concentrated rod network describes the structure of the SWNTs in the linear viscoelastic regime. (d) The structure of the network during the loss of rigidity.

moduli-strain curves so the yield strain for all samples occurs at the same ''rescaled'' strain. The scaling provides a clue to the underlying microscopic mechanism for strain induced fluidization.

In order for strain induced fluidization to occur, each rod must debond from its neighbors and disentangle from the network. This simple fluidization criterion is based on microscale rod network motions [see Figs. 3(c) and 3(d)]. For small shear [e.g., in the x direction, Fig. 3(c)], network deformation is small and elastic, corresponding to the linear regime of the network viscoelasticity. The response becomes nonlinear when the bonds between the nanotubes break, i.e., when the nanotubes rotate through angles with arc length larger than the bond interaction range [$R_{\min} \approx 1.7$ nm for two (10,10) carbon nanotubes [9]]. At the onset of fluidization ($G'' > G'$), the network is destroyed because the nanotubes have rotated through angles large enough to disentangle the tubes from one another [Fig. 3(d)]. We note that, in contrast to recent simulations suggesting network deformation is nonaffine near the percolation threshold [25], we have assumed the deformation is affine in this analysis, thus implying the fluidization criteria is independent of the stiffness of the SWNTs.

The maximum angle before fluidization depends only on the microscopic geometry of the network [see Fig. 3(d)]. In other words, the arc length of the maximum angle is approximately the length of the rod, the diameter of the rod, or the mesh size of the network. The mesh size is the only length scale that agrees with the scaling found empirically. We suggest the maximum angle a rod can rotate before fluidization is approximately

$$\tan\theta_{\max} \approx \xi/\sqrt{L^2 - \xi^2}, \tag{1}$$

where L is the nanotube length and D_{eff} is the effective diameter of the nanotube with its surfactant layer. The mesh size of the network, $\xi = \sqrt{3/2\phi}D_{\text{eff}}$, is taken to be the lattice constant of a cubic lattice formed by overlapping rods [26,27]. The expression for $\theta_{\max}$ is valid provided that $R_{\min} < \xi$. Note, $\tan\theta_{\max}$ reflects the microscopic structure of the network. If the network structure were unimportant, then we would expect $\tan\theta_{\max}$ independent of volume fraction. We can write Eq. (1) as a function of $(\phi - \phi^*)$ because $\xi(\phi = \phi^*) \approx L \approx D_{\text{eff}}/\sqrt{\phi^*}$ at the onset of rigidity percolation, i.e.,

$$\tan\theta_{\max} \approx \frac{1/\sqrt{\phi}}{\sqrt{1/\phi^* - 1/\phi}} = \left(\frac{\phi^*}{\phi - \phi^*}\right)^{1/2}. \tag{2}$$

Replacing $\sqrt{\phi^*}$ with D_{eff}/L in Eq. (2) gives $\tan\theta_{\max} \approx D_{\text{eff}}/L(\phi - \phi^*)^{1/2}$. Since $\tan\theta$ equals the macroscopic strain ϵ, $\tan\theta_{\max}$ defines the macroscopic yield strain ϵ_y at fluidization, and we recover the scaling relation found empirically. The model suggests that far above the percolation threshold, the fluidization strain will scale as $\phi^{-1/2}$. Thus the more tightly packed carbon nanotube networks yield more easily. A similar scaling relation was shown for cross-linked actin solutions [1], but for a physically different reason. Polymers such as actin yield because of the stretching of individual filaments before breakage [28].

In Fig. 4(a) we show the stress σ measured at 1 Hz as a function of the strain ϵ for various ϕ. Notice σ increases linearly with ϵ and then reaches a plateau for all volume fractions except $\phi = 0.003$. The plateau is indicative of a yielding event. Assuming the loss of rigidity occurs after the nanotubes disassociate from their neighbors, these yield stresses σ_y can be used to estimate the interaction energy between the rods [23]. This type of analysis has been used with success to infer the attractive interactions energies in colloidal gels [29]. In order to apply this analysis, we must eliminate the volume fraction dependence from the stress so the scaled plateau stress will be proportional to the bond energy [29]. We find empirically it is possible to eliminate the ϕ dependence of the stress by multiplying σ by a scale factor proportional to $(\phi - \phi^*)^{-3/2}$ [Fig. 4(b)]. The scaling of the stress can be most easily understood in terms of bonding in the network. In the concentrated limit ($\phi \gg \phi^*$) the number density of bonds is proportional to $1/\xi^3 \propto \phi^{3/2}$. Therefore, we can eliminate the concentration dependence of σ with a scale factor proportional to $\phi^{-3/2}$, provided the bond interaction energy is independent of the volume fraction [30].

We generate a master curve for all stress-strain data by scaling the strain by $(L/D_{\text{eff}})(\phi - \phi^*)^{1/2}$ (which accounts for the microscopic reorganization of the network) as before, and scaling the stress by $(V_{\text{rod}}/k_BT) \times (\phi - \phi^*)^{-3/2}$ (which accounts for the bond density of

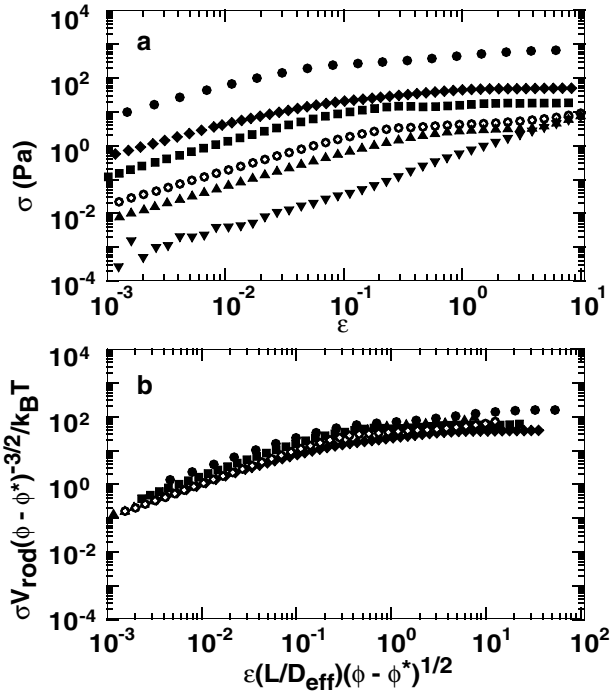

FIG. 4. (a) Volume fraction ϕ dependent stress σ versus strain ϵ at 1 Hz for SWNT suspensions. Circles, diamonds, squares, circles with dot, up triangles, and down triangles are for $\phi =$ 0.03, 0.015, 0.0075, 0.005, 0.004, and 0.003, respectively. (b) Master curve of scaled σ versus scaled ϵ.

the network), where V_{rod} is the volume of a surfactant coated nanotube [Fig. 4(b)]. Note, *a priori* we could have chosen other volumes in the stress prefactor, e.g., D_{eff}^3, $D_{\text{eff}}L^2$, or L^3; however, these other prefactors gave unphysically large or small bond energies, and therefore were discarded. When cast in this dimensionless form, the plateau of the scaled stress corresponds to the energy per volume of rod in units of k_BT and gives a bond interaction energy, $E_{\text{bond}} \approx 40k_BT$. The scaling implies the yield stress is given by $\sigma_y \approx E_{\text{bond}}(\phi - \phi^*)^{3/2}/V_{\text{rod}}$. If we assume that the bonding occurs due to the van der Waals interaction across the diameter of a SWNT (~ 1 nm), the estimated E_{bond} agrees with the theoretical prediction for the interaction energy between bare (10,10) SWNTs [9].

We use the expressions for σ_y and ϵ_y to express the linear elasticity in terms of the interaction energy, $G' \approx \sigma_y/\epsilon_y \approx (\phi - \phi^*)^2 E_{\text{bond}}/D_{\text{eff}}^3$. The ϕ dependence of this expression is in agreement with experiment (Fig. 2). For $\phi = 0.03$, this expression gives $G' \approx 2000$ Pa, in agreement with the measured elasticity of nanotube networks (Fig. 1). If the elasticity were to originate from the bending or stretching of individual tubes, for the same ϕ we would expect $G'_{\text{bending}} \approx k_BTl_p/\xi^4 \approx 5 \times 10^4$ Pa [31] and $G'_{\text{stretching}} \approx k_BTl_p^2/\xi^5 \approx 4 \times 10^7$ Pa [28].

In conclusion, we have measured the linear and nonlinear viscoelasticity of SWNT suspensions. The rod networks exhibit rigidity percolation but differ from other semiflexible filament networks in that the elasticity appears to be due to the bonding (rather than stretching or bending) of the rods. The data suggest SWNTs in suspension form elastic networks held together by freely jointed bonds of interaction energy $\approx 40k_BT$.

We gratefully acknowledge useful conversations with Tom Lubensky and Brian DiDonna. This work has been partially supported by the NSF (MRSEC DMR-00-79909 AGY, PAJ; DMR-0203378 AGY), NASA (NAG8-2172 AGY), and the NIH (GM56707 PAJ). The data were taken in the Viscoelastic Characterization Facility within the MRSEC at the University of Pennsylvania.

[1] M. L. Gardel *et al.*, Science **304**, 1301 (2004).
[2] S. Lin-Gibson *et al.*, Phys. Rev. Lett. **92**, 048302 (2004).
[3] V. A. Davis *et al.*, Macromolecules **37**, 154 (2004).
[4] E. S. Choi *et al.*, J. Appl. Phys. **94**, 6034 (2003).
[5] A. B. Dalton *et al.*, Nature (London) **423**, 703 (2003).
[6] M. F. Islam *et al.*, Phys. Rev. Lett. **92**, 088303 (2004).
[7] l_p is estimated using $l_p = YI/k_BT$, where $Y \sim 1.25$ TPa is the Young's modulus [8], and $I = \pi D^4/64$.
[8] M. M. J. Treacy *et al.*, Nature (London) **381**, 678 (1996).
[9] L. A. Girifalco *et al.*, Phys. Rev. B **62**, 13 104 (2000).
[10] M. F. Islam *et al.*, Nano Lett. **3**, 269 (2003).
[11] T.W. Odom *et al.*, Nature (London) **391**, 62 (1998).
[12] J. Hone *et al.*, Phys. Rev. B **59**, R2514 (1999).
[13] M. Sahimi and S. Arbabi, Phys. Rev. B **47**, 703 (1993).
[14] M. F. Islam *et al.*, Phys. Rev. Lett. **93**, 037404 (2004).
[15] W. Zhou *et al.*, Chem. Phys. Lett. **384**, 185 (2004).
[16] $\bar{\phi} = 3D_{\text{eff}}^2/2L^2 = 0.0014$, where $D_{\text{eff}} = 5.1$ nm and $L =$ 165 nm [17]. This is the minimum volume fraction of rods needed to form a connected network.
[17] M. Doi and S. F. Edwards, *The Theory of Polymer Dynamics* (Claredon, Oxford, 1992).
[18] S. P. Obukhov, Phys. Rev. Lett. **74**, 4472 (1995).
[19] Because some SWNT concentrations are far from the percolation threshold, experiments are in progress to obtain G'_0 near ϕ^* to validate the value of ν.
[20] D. A. Head *et al.*, Phys. Rev. E **68**, 025101 (2003).
[21] D. A. Head *et al.*, Phys. Rev. Lett. **91**, 108102 (2003).
[22] J. Wilhelm and E. Frey, Phys. Rev. Lett. **91**, 108103 (2003).
[23] The yield strain (or yield stress) is defined such that it occurs at the onset of fluidization ($G'' = G'$).
[24] P. Sollich *et al.*, Phys. Rev. Lett. **78**, 2020 (1998), and references therein.
[25] D. A. Head *et al.*, Phys. Rev. E **68**, 061907 (2003).
[26] P. DeGennes *et al.*, J. Phys. (Les Ulis) **37**, 1461 (1976).
[27] C. F. Schmidt *et al.*, Macromolecules **22**, 3638 (1989).
[28] F. C. MacKintosh *et al.*, Phys. Rev. Lett. **75**, 4425 (1995).
[29] W. B. Russel, D. A. Saville, and W. R. Schowalter, *Colloidal Dispersions* (Cambidge University Press, Cambridge, 1989).
[30] A similar master curve was found for a SWNT:NaDDBS ratio of 1:10.
[31] K. Kroy and E. Frey, Phys. Rev. Lett. **77**, 306 (1996).